The Canadian Mineralogist
Vol. 60, pp. 837-847 (2022)
DOI: 10.3749/canmin.2200013

DONDOELLITE, $Ca_2Fe(PO_4)_2{\cdot}2H_2O$, A NEW MINERAL SPECIES POLYMORPHIC WITH MESSELITE, FROM RAPID CREEK, YUKON, CANADA

HEXIONG YANG[§], RONALD B. GIBBS, JAMES A. MCGLASSON, ROBERT A. JENKINS, AND ROBERT T. DOWNS

Department of Geosciences, University of Arizona, 1040 E. 4th Street, Tucson, Arizona 85721-0077, USA

ABSTRACT

A new mineral species, dondoellite, ideally $Ca_2Fe(PO_4)_2{\cdot}2H_2O$, was found in the Grizzly Bear Creek, Dawson mining district, Yukon, Canada. It is polymorphic with messelite, a member of the fairfieldite group. Dondoellite occurs as spherical aggregates (diameters up to 2 cm) of radiating bladed crystals. Associated minerals include hydroxylapatite, siderite, and quartz. No twinning or parting is observed. The mineral is colorless to pale yellow in transmitted light, is transparent with white streak, and has vitreous luster. It is brittle and has a Mohs hardness of 3½–4, with perfect cleavage on {001}. The measured and calculated densities are 3.14(5) and 3.15 g/cm^3, respectively. Optically, dondoellite is biaxial (+), with $\alpha = 1.649(5)$, $\beta = 1.654(5)$, $\gamma = 1.672(5)$ (white light), 2V (meas.) = 55(2)°, 2V (calc.) = 58°. An electron probe microanalysis yields an empirical formula (based on 10 O *apfu*) $Ca_{1.99}(Fe_{0.89}Mg_{0.13}Mn_{0.01})_{\Sigma 1.03}(P_{1.00}O_4)_2{\cdot}2H_2O$, which can be simplified to $Ca_2(Fe^{2+},Mg,Mn^{2+})(PO_4)_2{\cdot}2H_2O$.

Dondoellite is triclinic, space group $P\bar{1}$, $a = 5.4830(2)$, $b = 5.7431(2)$, $c = 13.0107(5)$ Å, $\alpha = 98.772(2)$, $\beta = 96.209(2)$, $\gamma = 108.452(2)°$, $V = 378.71(2)$ Å^3, and $Z = 2$. The crystal structure of dondoellite is characterized by isolated $FeO_4(H_2O)_2$ octahedra that are linked by corner-sharing with PO_4 tetrahedra to form so-called kröhnkite-type $[Fe(PO_4)_2(H_2O)_2]^{2-}$ chains along [100], similar to that observed in messelite. These chains are connected to one another by large Ca^{2+} cations and H bonds to form layers parallel to (001). The layers are further linked together by Ca–O and H bonds. However, unlike messelite, the crystal structure of dondoellite contains two symmetrically independent PO_4 tetrahedra ($P1O_4$ and $P2O_4$) and two distinct $CaO_7(H_2O)$ polyhedra (Ca1 and Ca2). The kröhnkite-type chains in dondoellite are constructed with $P1O_4$ tetrahedra on one side and $P2O_4$ tetrahedra on the other. Topologically, the dondoellite structure can be considered a combination of the collinsite and messelite structures alternating along [001], thus representing a new structure type for minerals with kröhnkite-type chains. The discovery of dondoellite raises the question as to whether polymorphs of fairfieldite, $Ca_2Mn^{2+}(PO_4)_2{\cdot}2H_2O$, or collinsite, $Ca_2Mg(PO_4)_2{\cdot}2H_2O$, might also be found in nature.

Keywords: dondoellite, messelite, fairfieldite, new mineral, crystal structure, Yukon.

INTRODUCTION

Dondoellite, ideally $Ca_2Fe(PO_4)_2{\cdot}2H_2O$, is a new mineral found on specimens collected from the Grizzly Bear Creek, Stoneman Camp (Area B; Area 2), Rapid Creek, Dawson mining district, Yukon, Canada. It is named in honor of both Dr. Donald V. Doell (father, born in 1948) and Dr. Donald M. Doell (son, born in 1982). Don V. Doell received his M.D. from McGill University in 1973 and is one of the principal investigators in a study on mesothelioma and mineral exposure, combing his interest in mineralogy with medicine. He has been collecting minerals since his childhood, eventually becoming the principal supplier of mineral specimens from the quarry in St. Michel on Montreal Island (weloganite, dawsonite, cryolite) to collectors and museums around the world. Don V. Doell is a major contributor to The Canadian Museum of Nature collection with special recognition as a Collections Patron. He has chaired fundraising campaigns and helped the museum acquire significant mineral collections, such as the William Pinch collection and the Gilles Haineault collection of mineral specimens from Mont Saint Hilaire. Don M. Doell received his M.D. from McGill University in 2006 and is currently a specialist in internal and geriatric medicines at McGill. He began his interest in

---

[§] *Corresponding author e-mail address:* hyang@arizona.edu minerals by attending mineral shows with his parents as a toddler and developed a passion for field collecting. Don M. Doell has a special interest in pegmatite mineralogy, especially phosphates, and mineralogy from alkaline deposits, such as Mount Saint Hilaire and Mount Malosa.

Together, Don V. Doell and Don M. Doell have supported research into mineralogy and geology while trying to bridge the passion that exists among amateur enthusiasts and collectors and the academic world. They are especially interested in supporting museums (such as The Redpath Museum at McGill University in Montreal and The Mineral Museum in Bancroft, Ontario) to help preserve this important natural heritage and better understand our planet. In the past 10 years, Don V. Doell and Don M. Doell have donated 173 mineral specimens to the RRUFF Database at the University of Arizona (http://rruff.info) for data collection and research. The new mineral and its name have been approved by the Commission on New Minerals, Nomenclature and Classification (CNMNC) of the International Mineralogical Association (IMA 2021-041). The cotype samples have been deposited at the University of Arizona Alfie Norville Gem and Mineral Museum (Catalogue # 22710) and the RRUFF Project (deposition # R210003) (http://rruff.info). This paper describes the physical and chemical properties of dondoellite and its crystal structure determined from single-crystal X-ray diffraction data, illustrating its structural relationships to messelite in particular and minerals with kröhnkite-type chains in general.

SAMPLE DESCRIPTION AND EXPERIMENTAL METHODS

Occurrence, physical and chemical properties, and Raman spectra

Dondoellite was found on specimens collected from the Grizzly Bear Creek, Stoneman Camp (Area B; Area 2) (68° N, 137° W, est.), Rapid Creek, Dawson mining district, Yukon, Canada. Associated minerals are hydroxylapatite, siderite, and quartz. The host rock at the Rapid Creek type locality is a sedimentary iron formation with marine phosphorites and shales (Robinson *et al.* 1992). Dondoellite and associated minerals are found as fracture fillings in the quartz-phosphate veins. The fracture-filling minerals most likely formed during or after the Laramide Orogeny, which tilted and fractured the host rock, creating open space for fluids to enter and precipitate the observed mineral assemblage. The pressure and temperature conditions prevalent during the vent were probably in the uppermost range of diagenesis to the lowermost range of regional metamorphism. Based on direct evidence from fluid inclusions, the formation temperature of the quartz-phosphate veins must have been at least 180–200 °C (Robinson *et al.* 1992). As for dondoellite, its formation temperature was estimated to range from 50 to 200 °C, the lowest among all fracture-filling phosphates.

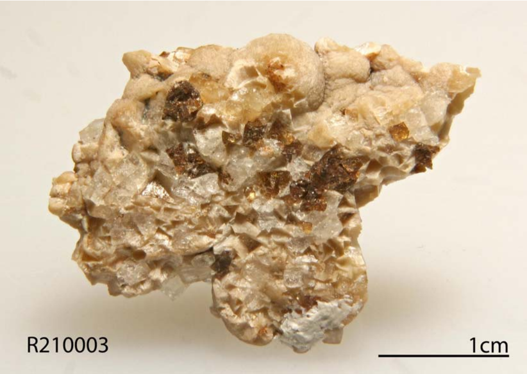

FIG. 1. The specimen on which dondoellite was found.

Dondoellite occurs as spherical aggregates (diameters up to 2 cm) of radiating bladed white to straw-yellow or tan crystals, on top of orange-brown siderite and white hydroxylapatite (Figs. 1 and 2). Individual crystals of dondoellite are up to 0.80 × 0.10 × 0.03 mm in size. No twinning or parting is observed macroscopically. The mineral is colorless to pale yellow in transmitted light, is transparent with white streak, and has vitreous luster. It is brittle and has a Mohs hardness of 3½–4, with perfect cleavage on {001}. The density measured by flotation in heavy liquids is 3.14(5) g/cm^3 and the calculated density is 3.15 g/cm^3. Optically, dondoellite is biaxial (+), with $\alpha = 1.649(5)$, $\beta = 1.654(5)$, $\gamma = 1.672(5)$ (white light), $2V$ (meas.) = 55(2)°, $2V$ (calc.) = 58°. The pleochroism is weak, from gray to light yellow, and the dispersion is

FIG. 2. A microscopic view of white to straw-yellow or tan radiating bladed crystals dondoellite.

TABLE 1. THE CHEMICAL COMPOSITION OF DONDOELLITE (IN wt.%)

Constituent	Mean	Range	Stand. Dev.	Probe Standard
P_2O_5	39.22	38.73–39.79	0.33	Synthetic apatite
CaO	30.93	30.59–31.38	0.22	Synthetic apatite
FeO	17.82	17.57–18.18	0.24	Fayalite
MgO	1.51	1.37–1.64	0.08	Diopside
MnO	0.24	0.14–0.40	0.08	Rhodonite
H_2O_{calc}	10.02			Added in ideal value
Total	99.74	98.88–100.66	0.59	

Note: The H_2O content was calculated assuming $2H_2O$.

weak, with $r > v$. The calculated compatibility index based on the empirical formula is 0.006 (superior) (Mandarino 1981). Dondoellite is insoluble in water or hydrochloric acid.

The chemical composition was determined using a Cameca SX-100 electron microprobe (WDS mode, 15 kV, 10 nA, and a beam diameter of 5 μm). The standards used for the probe analysis are given in Table 1, along with the determined compositions (9 analysis points). The resultant chemical formula, calculated on the basis of 10 O atoms *pfu* (from the structure determination), is $Ca_{1.99}(Fe_{0.89}Mg_{0.13}Mn_{0.01})_{\Sigma 1.03}(P_{1.00}O_4)_2 \cdot 2H_2O$, which can be simplified to $Ca_2(Fe,Mg)(PO_4)_2 \cdot 2H_2O$.

The Raman spectrum of dondoellite (Fig. 3) was collected on a randomly oriented crystal with a Thermo Almega microRaman system, using a solid-state laser with a wavelength of 532 nm at the full power of 150 mW and a thermoelectric cooled CCD detector. The laser is partially polarized with 4 cm^{-1} resolution and a spot size of 1 μm.

X-ray crystallography

Both the powder and single-crystal X-ray diffraction data for dondoellite were collected using a Bruker X8 APEX2 CCD X-ray diffractometer equipped with graphite-monochromatized Mo$K\alpha$ radiation. The measured powder X-ray diffraction data, along with those calculated from the determined structure using the program XPOW (Downs *et al*. 1993) are given in Table 2. The unit-cell parameters refined from the powder X-ray diffraction data are $a = 5.479(2)$, $b = 5.7388(16)$, $c = 13.004(4)$ Å, $\alpha = 98.81(3)°$, $\beta = 96.17(3)°$, $\gamma = 108.43(3)°$, and $V = 377.98(15)$ Å^3.

Single-crystal X-ray diffraction data of dondoellite were collected from a nearly equidimensional crystal (0.06 × 0.06 × 0.05 mm) with frame widths of 0.5° in ω and 30 s counting time per frame. All reflections were indexed on the basis of a triclinic unit cell (Table 3). Intensity data were corrected for X-ray absorption using the Bruker program SADABS. The systematic absences of reflections suggest the possible space group $P1$ or $P\bar{1}$. The crystal structure was solved and refined using SHELX2018 (Sheldrick 2015a, 2015b). All H atoms were located through the difference Fourier syntheses. For simplicity, the small amount of Mn was treated as Fe and the chemical formula $Ca_2(Fe_{0.87}Mg_{0.13})(PO_4)_2 \cdot 2H_2O$ was used during the structure refinements. All non-H atoms were refined anisotropically, whereas all H atoms were only refined

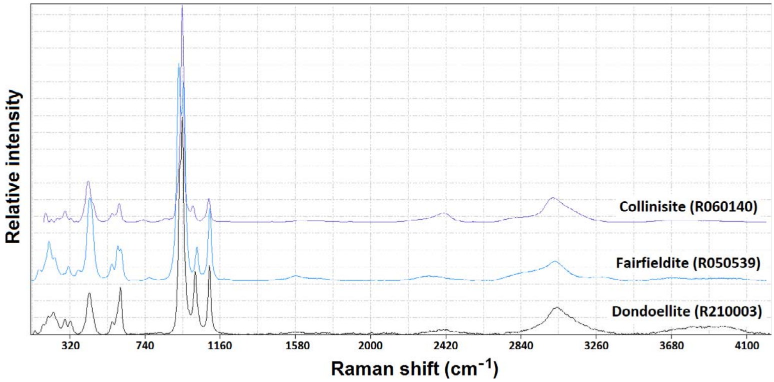

FIG. 3. Raman spectra of dondoellite, fairfieldite, and collinsite.

TABLE 2. POWDER X-RAY DIFFRACTION DATA OF DONDOELLITE

I	d_{obs}	d_{cal}	*h*	*k*	*l*
35	6.316	6.336	0	0	2
8	5.013	5.052	$\bar{1}$	0	1
15	4.590	4.602	0	1	1
10	4.489	4.498	1	0	1
15	3.731	3.733	0	1	2
15	3.724	3.731	1	$\bar{1}$	2
17	3.559	3.563	$\bar{1}$	0	3
22	3.254	3.276	$\bar{1}$	$\bar{1}$	1
100	3.149	3.149	$\bar{1}$	$\bar{1}$	2
63	3.023	3.022	1	0	3
18	2.871	2.875	$\bar{1}$	$\bar{1}$	3
24	2.789	2.784	$\bar{1}$	2	0
100	2.669	2.666	1	$\bar{2}$	2
26	2.628	2.628	1	1	2
30	2.574	2.573	$\bar{1}$	1	4
15	2.460	2.460	1	$\bar{2}$	3
7	2.352	2.352	$\bar{2}$	1	3
20	2.226	2.224	1	$\bar{2}$	4
15	2.196	2.198	2	$\bar{1}$	3
20	2.131	2.131	0	1	5
21	2.098	2.099	$\bar{2}$	$\bar{1}$	1
10	2.081	2.077	0	2	3
10	2.019	2.019	2	$\bar{2}$	3
8	1.980	1.980	2	$\bar{1}$	4
10	1.964	1.964	2	1	1
8	1.931	1.931	1	$\bar{1}$	6
10	1.867	1.868	1	2	2
15	1.829	1.830	$\bar{1}$	3	1
10	1.804	1.804	$\bar{1}$	0	7
25	1.782	1.782	$\bar{2}$	0	6
25	1.701	1.702	0	$\bar{3}$	4
22	1.684	1.684	$\bar{3}$	0	3
10	1.668	1.668	$\bar{2}$	3	2
17	1.659	1.659	0	$\bar{2}$	7
8	1.637	1.637	$\bar{1}$	3	3
5	1.606	1.605	1	1	6
5	1.582	1.584	0	0	8
7	1.558	1.558	$\bar{1}$	$\bar{3}$	1
6	1.513	1.512	$\bar{2}$	$\bar{2}$	5
8	1.454	1.453	2	$\bar{1}$	7
5	1.414	1.414	2	$\bar{3}$	6
10	1.395	1.395	2	2	3

isotropically. Final atomic coordinates and displacement parameters for dondoellite are given in Tables 4 and 5, respectively. Selected bond distances are presented in Table 6 and hydrogen bonds in Table 7.

Crystal Structure Description and Discussion

Dondoellite is a dimorph of $Ca_2Fe^{2+}(PO_4)_2{\cdot}2H_2O$, the other being messelite. The crystal structure of dondoellite is characterized by isolated $FeO_4(H_2O)_2$ octahedra that are linked by corner-sharing with PO_4 tetrahedra to form $[Fe(PO_4)_2(H_2O)_2]^{2-}$ chains infinite along [100] (Fig. 4), similar to that in messelite (Fleck & Kolitsch 2003). Chains with octahedra corner-linked to tetrahedra have been found in a number of compounds and have been referred to as kröhnkite-type chains (see Fleck *et al.* 2002a for a detailed review). The $[Fe(PO_4)_2(H_2O)_2]^{2-}$ chains in dondoellite are connected to one another by large Ca^{2+} cations and H bonds to form layers parallel to (001). The layers are further linked together by Ca–O and hydrogen bonds (Figs. 5 and 6).

The crystal structure of messelite contains ten symmetrically independent atoms (one Ca, one Fe, one P, five O, and two H atoms; Fleck & Kolitsch 2003), which is different than that in the crystal structure of dondoellite, which contains 19 symmetrically independent atoms: two Ca, one Fe, two P, ten O, and four H atoms, giving rise to two distinct $CaO_7(H_2O)$ polyhedra (Ca1 and Ca2), two PO_4 tetrahedra ($P1O_4$ and $P2O_4$), and one $FeO_4(H_2O)_2$ octahedron. The kröhnkite-type $[Fe(PO_4)_2(H_2O)_2]^{2-}$ chains in dondoellite are formed by the $P1O_4$ tetrahedra on one side and the $P2O_4$ tetrahedra on the other (Figs. 4, 5, and 6).

Fleck *et al.* (2002a) presented a thorough review of both minerals and synthetic compounds with kröhnkite-type chains and divided them into six different structure types (Types A to F). Type A is triclinic ($P\bar{1}$) and includes collinsite, talmessite, cassidyite, parabrandtite, roselite-β, and gaitite; Type B is also triclinic ($P\bar{1}$) and includes fairfieldite and messelite. The kröhnkite-type chains and their linkage to layers are identical in Type A and Type B materials, but the stacking of the layers is different: Two adjacent layers are shifted with respect to each other by *a*/2 for Type B materials, resulting in their γ-angle being close to 90° (Fleck *et al.* 2002a). Type D is monoclinic ($P2_1/c$) and includes wendwilsonite, brandtite, roselite, zincroselite, rruffite, and kröhnkite. Thus far, all materials in Types C, E, and F are only known as synthetic compounds. Noticeably, among all materials with kröhnkite-type chains, dondoellite is the first mineral that possesses two symmetrically distinct tetrahedral groups. Its structure does not belong to any of the six structure types summarized by Fleck *et al.* (2002a), thus representing a new structure type for such materials. It should be noted that the synthetic compounds $K_2Cd(SeO_4)_2{\cdot}2H_2O$ (Peytavin *et al.* 1974, Fleck *et al.* 2002b) and $K_2Mn(SO_4)_2{\cdot}2H_2O$ (Fleck *et al.* 2002b), both belong to the Type C class and contain two symmetrically distinct tetrahedra in their structures, but the linkage involving the octahedra to form the kröhnkite-type chains is different from that in dondoellite (Figs. 4, 5, and 6).

TABLE 3. SUMMARY OF CRYSTALLOGRAPHIC DATA AND REFINEMENT RESULTS FOR DONDOELLITE

	Messelite	Dondoellite
Ideal chemical formula	$Ca_2Fe^{2+}(PO_4)_2\cdot 2H_2O$	$Ca_2Fe^{2+}(PO_4)_2\cdot 2H_2O$
Crystal symmetry	Triclinic	Triclinic
Space group	$P\bar{1}$	$P\bar{1}$
a (Å)	5.480(1)	5.4830(2)
b (Å)	5.759(1)	5.7431(2)
c (Å)	6.569(1)	13.0107(5)
α (°)	90.18(3)	98.772(2)
β (°)	102.62(3)	96.209(2)
γ (°)	108.45(3)	108.452(2)
V (Å^3)	191.3(1)	378.71(2)
Z	1	2
ρ_{cal}(g/cm^3)	3.11	3.12
2θ range for data collection	$\leq$60	$\leq$65.15
No. of reflections collected	2062	9693
No. of independent reflections	1115	2607
No. of reflections with $I > 2\sigma(I)$	1074	2173
No. of parameters refined	81	153
R(int)		0.021
Final R_1, wR_2 factors [$I > 2\sigma(I)$]	0.022, 0.058	0.034, 0.087
Goodness-of-fit		1.080
Mineral locality	"Leithorizont M", Messel Oil Shale, Darmstadt, Germany	Rapid Creek, Yukon, Canada
Reference	Fleck *et al*. (2003)	This study

TABLE 4. FRACTIONAL ATOMIC COORDINATES AND EQUIVALENT ISOTROPIC DISPLACEMENT PARAMETERS (Å^2) FOR DONDOELLITE

Atom	x	y	z	U_{iso}*/U_{eq}	Occ. (<1)
Ca1	0.47254 (9)	−0.13574 (8)	0.12625 (3)	0.00847 (10)	
Ca2	0.03193 (9)	0.81040 (8)	0.36342 (3)	0.00755 (10)	
Fe	0.26002 (6)	0.34177 (6)	0.25395 (3)	0.00691 (10)	0.87
Mg	0.26002 (6)	0.34177 (6)	0.25395 (3)	0.00691 (10)	0.13
P1	−0.20943 (11)	0.50442 (10)	0.12703 (4)	0.00511 (12)	
P2	0.71723 (11)	0.17007 (10)	0.36517 (4)	0.00513 (12)	
O1	−0.3815 (3)	0.5484 (3)	0.21037 (13)	0.0098 (3)	
O2	0.0755 (3)	0.5842 (3)	0.18679 (13)	0.0086 (3)	
O3	−0.3041 (3)	0.2372 (3)	0.06450 (13)	0.0090 (3)	
O4	−0.2220 (3)	0.6905 (3)	0.05439 (13)	0.0100 (3)	
O5	0.4278 (3)	0.0740 (3)	0.30949 (12)	0.0087 (3)	
O6	0.8840 (3)	0.1189 (3)	0.28079 (13)	0.0100 (3)	
O7	0.7550 (3)	0.0123 (3)	0.44811 (12)	0.0081 (3)	
O8	0.7980 (3)	0.4462 (3)	0.41475 (12)	0.0086 (3)	
OW9	0.1814 (3)	0.0988 (3)	0.11000 (13)	0.0085 (3)	
OW10	0.3334 (3)	0.5888 (3)	0.39893 (13)	0.0094 (3)	
H1	0.202 (6)	0.181 (6)	0.060 (3)	0.014 (8)*	
H2	0.065 (9)	−0.004 (8)	0.097 (3)	0.034 (12)*	
H3	0.458 (9)	0.698 (8)	0.416 (3)	0.037 (12)*	
H4	0.267 (7)	0.537 (7)	0.452 (3)	0.029 (10)*	

TABLE 5. ATOMIC DISPLACEMENT PARAMETERS (Å^2) FOR DONDOELLITE

Atom	U^{11}	U^{22}	U^{33}	U^{12}	U^{13}	U^{23}
Ca1	0.0097 (2)	0.0089 (2)	0.0083 (2)	0.00424 (17)	0.00242 (15)	0.00288 (15)
Ca2	0.0079 (2)	0.00719 (19)	0.0081 (2)	0.00282 (16)	0.00207 (15)	0.00209 (15)
Fe	0.00702 (17)	0.00686 (17)	0.00701 (17)	0.00211 (13)	0.00228 (12)	0.00160 (12)
Mg	0.00702 (17)	0.00686 (17)	0.00701 (17)	0.00211 (13)	0.00228 (12)	0.00160 (12)
P1	0.0048 (2)	0.0049 (2)	0.0047 (2)	0.0008 (2)	0.00008 (18)	0.00080 (18)
P2	0.0046 (2)	0.0051 (2)	0.0051 (2)	0.0010 (2)	0.00018 (18)	0.00122 (18)
O1	0.0105 (7)	0.0108 (7)	0.0093 (7)	0.0043 (6)	0.0042 (6)	0.0025 (6)
O2	0.0058 (7)	0.0081 (7)	0.0093 (7)	0.0002 (6)	−0.0022 (6)	0.0013 (6)
O3	0.0078 (7)	0.0067 (7)	0.0098 (7)	0.0013 (6)	−0.0010 (6)	−0.0024 (5)
O4	0.0111 (8)	0.0097 (7)	0.0090 (7)	0.0024 (6)	0.0008 (6)	0.0040 (6)
O5	0.0059 (7)	0.0100 (7)	0.0083 (7)	0.0008 (6)	−0.0019 (6)	0.0019 (6)
O6	0.0108 (7)	0.0109 (7)	0.0091 (7)	0.0034 (6)	0.0046 (6)	0.0033 (6)
O7	0.0089 (7)	0.0088 (7)	0.0072 (7)	0.0036 (6)	0.0001 (6)	0.0029 (5)
O8	0.0098 (7)	0.0056 (7)	0.0084 (7)	0.0009 (6)	0.0006 (6)	−0.0004 (5)
OW9	0.0078 (8)	0.0085 (7)	0.0075 (7)	0.0007 (6)	0.0002 (6)	0.0020 (6)
OW10	0.0079 (8)	0.0112 (8)	0.0077 (8)	0.0019 (7)	0.0013 (6)	0.0006 (6)

TABLE 6. SELECTED BOND DISTANCES FOR DONDOELLITE

	Distance (Å)		Distance (Å)
Ca1–OW9	2.4046 (17)	Ca2–O8	2.3194 (17)
Ca1–O4	2.4056 (18)	Ca2–OW10	2.4314 (18)
Ca1–O3	2.4103 (17)	Ca2–O7	2.4394 (17)
Ca1–O3	2.4645 (16)	Ca2–O5	2.5006 (18)
Ca1–O1	2.5425 (17)	Ca2–O6	2.5006 (18)
Ca1–O2	2.5471 (17)	Ca2–O7	2.5060 (16)
Ca1–O5	2.5754 (17)	Ca2–O2	2.5359 (17)
Ca1–O6	2.7028 (17)	Ca2–O1	2.7053 (17)
Ave.	2.507	Ave.	2.488
Fe–OW9	2.0707 (17)		
Fe–OW10	2.0955 (17)		
Fe–O1	2.1359 (17)		
Fe–O6	2.1523 (17)		
Fe–O2	2.1900 (16)		
Fe–O5	2.1963 (17)		
Ave.	2.140		
P1–O3	1.5200 (17)	P2–O8	1.5195 (17)
P1–O4	1.5431 (17)	P2–O7	1.5481 (16)
P1–O1	1.5552 (17)	P2–O6	1.5546 (17)
P1–O2	1.5592 (17)	P2–O5	1.5565 (17)
Ave.	1.544	Ave.	1.545

TABLE 7. HYDROGEN-BOND GEOMETRY (Å, °) IN DONDOELLITE

D–H···*A*	*D*–H	H···*A*	*D*···*A*	*D*–H···*A*
O*W*9–H1···O4	0.85 (3)	1.76 (3)	2.609 (2)	172 (3)
O*W*9–H2···O4	0.70 (4)	1.91 (4)	2.601 (2)	172 (5)
O*W*10–H3···O7	0.75 (4)	1.96 (4)	2.705 (2)	171 (5)
O*W*10–H4···O8	0.86 (4)	1.81 (4)	2.621 (2)	157 (4)

A comparison of the crystal structures of collinsite (Brotherton *et al*. 1974, Herwig & Hawthorne 2006), messelite (Fleck & Kolitsch 2003), and dondoellite reveals that, topologically, the dondoellite structure can be considered a combination of the former two. As illustrated in Figure 7, linkages made between two kröhnkite-type chains for all three minerals involve Ca–O and H-bonds. A major difference between collinsite and messelite is that in collinsite (Brotherton *et al*. 1974, Herwig & Hawthorne 2006) only one (O4) of the two O atoms that are not shared by the $MO_4(H_2O)_2$ octahedra (M = Mg or Fe) participates in the H bonds, (forming *two* hydrogen bonds). The other O atom (O3) is not engaged in the H bond (Fig. 7a). This is contrast to what is observed in messelite (Fleck & Kolitsch 2003) where each of the two O atoms (O3 and O4) not shared by the octahedra participate in the H bonds (each forming one H bond) (Fig. 7b). In addition, although the Ca cations in the two minerals have a similar coordination ($7O + H_2O$), the average Ca–O bond in collinsite is longer (2.505 Å) than that in messelite (2.486 Å). Interestingly, the structure of dondoellite possesses both collinsite-type and messelite-type layers (Fig. 7c), the former developed by $P1O_4$, Ca1, and Ow9 (H_2O), and the latter by $P2O_4$, Ca2, and Ow10 (H_2O). In the collinsite-type layer in dondoellite, only O4 in the $P1O_4$ group is involved in the H bonds (acceptor for both H1 and H2) and the average Ca1–O bond length is 2.507 Å. In comparison, in the messelite-type layer in dondoellite, both O7 and O8 in the $P2O_4$ group are the H-bond acceptors (O7···H3 and O8···H4) and the average Ca2–O bond distance is 2.488 Å. These two types of layers alternate along [001] (Fig. 7c), giving

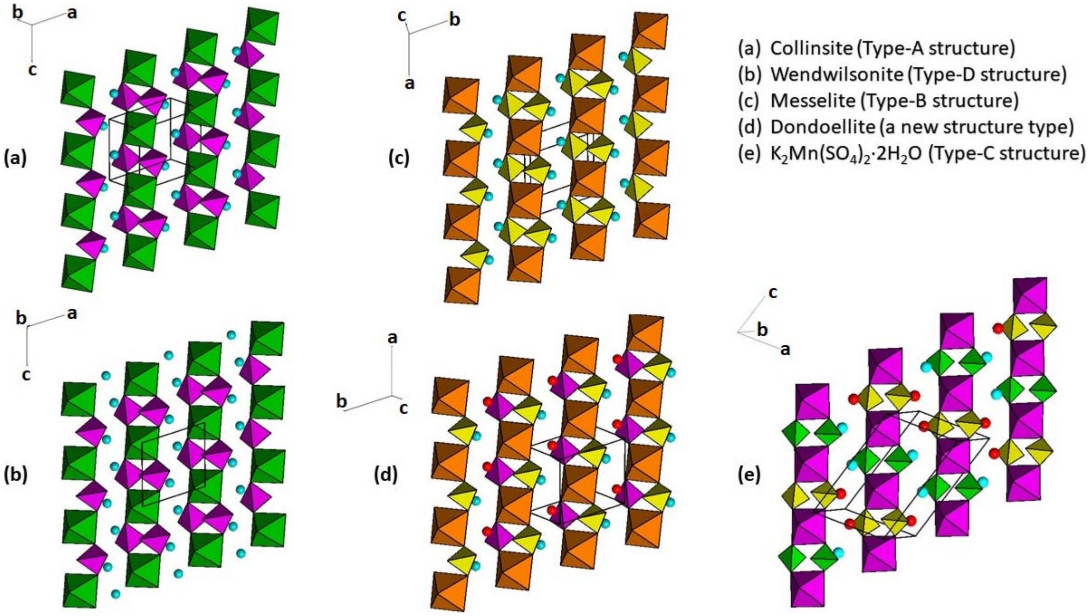

FIG. 4. A view of a polyhedral layer formed by vertically oriented kröhnkite-type chains linked together by Ca^{2+} or K^+ cations (spheres) in (a) collinsite (Herwig & Hawthorne 2006), (b) wendwilsonite (Kolitsch & Fleck 2006), (c) messelite (Fleck & Kolitsch 2003), (d) dondoellite (this study), and (e) $K_2Mn(SO_4)_2{\cdot}2H_2O$ (Fleck *et al*. 2002b). Tetrahedra represent PO_4, AsO_4, or SO_4, and octahedra MgO_6, FeO_6, or MnO_6. Two different colored spheres and tetrahedra in dondoellite and synthetic $K_2Mn(SO_4)_2{\cdot}2H_2O$ represent two symmetrically distinct Ca/K and PO_4/SO_4.

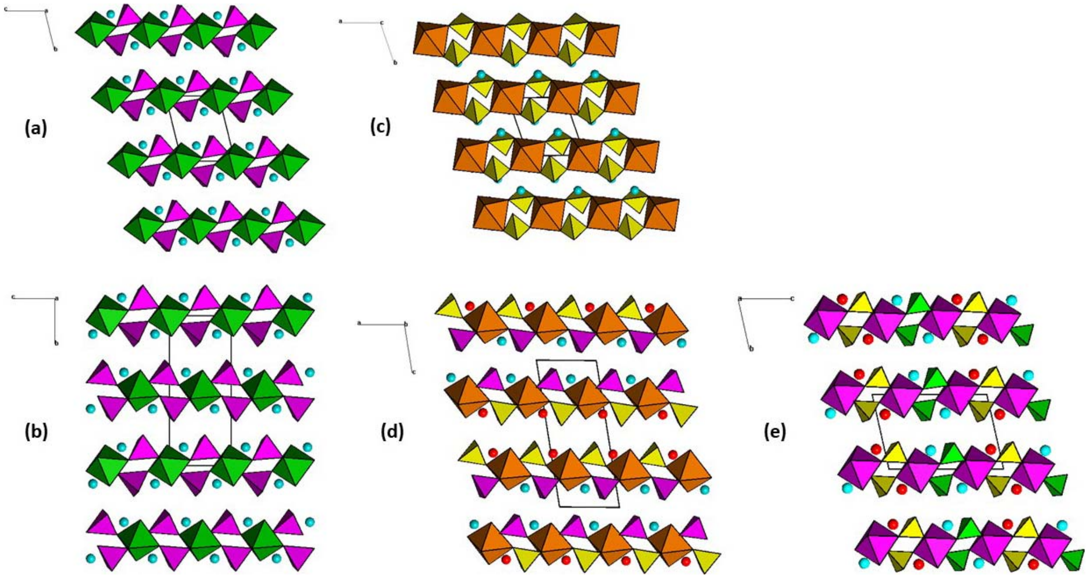

FIG. 5. A view parallel to polyhedral layers with horizontally oriented kröhnkite-type chains for (a) collinsite, (b) wendwilsonite, (c) messelite, (d) dondoellite, and (e) $K_2Mn(SO_4)_2{\cdot}2H_2O$. The legend is the same as in Figure 4.

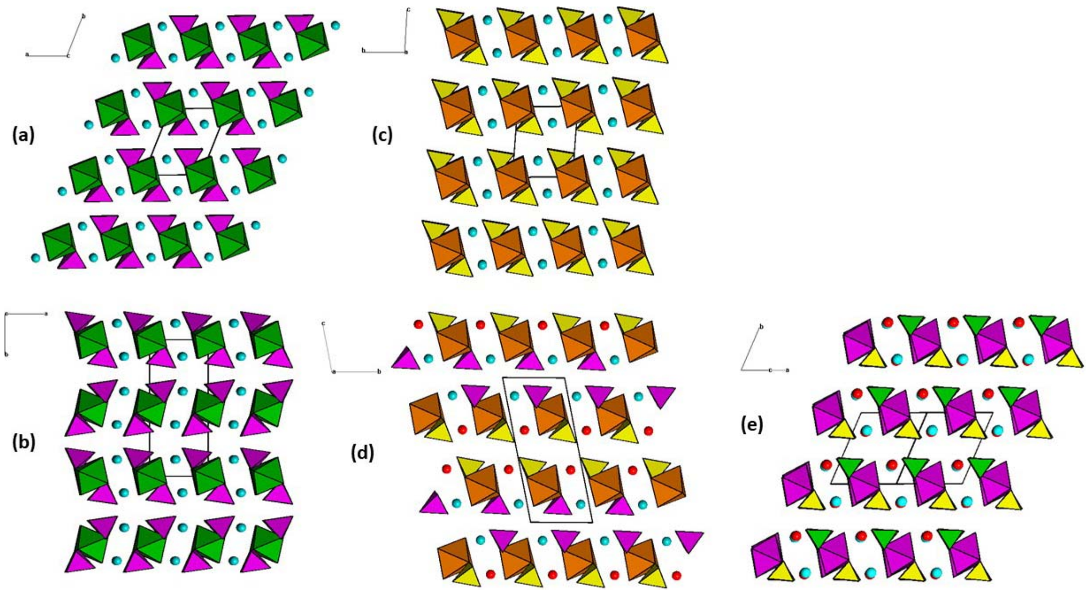

FIG. 6. A view parallel to polyhedral layers and along kröhnkite-type chains for (a) collinsite, (b) wendwilsonite, (c) messelite, (d) dondoellite, and (e) $K_2Mn(SO_4)_2{\cdot}2H_2O$. The legend is the same as in Figure 4.

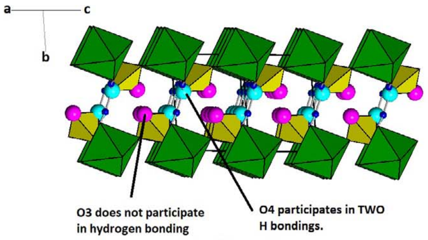

(a) Collinisite layer

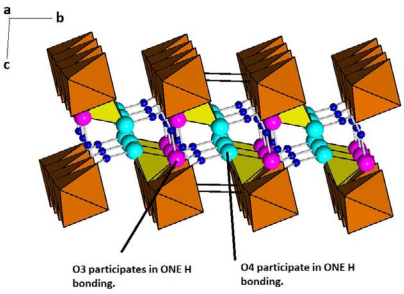

(b) Messelite layer

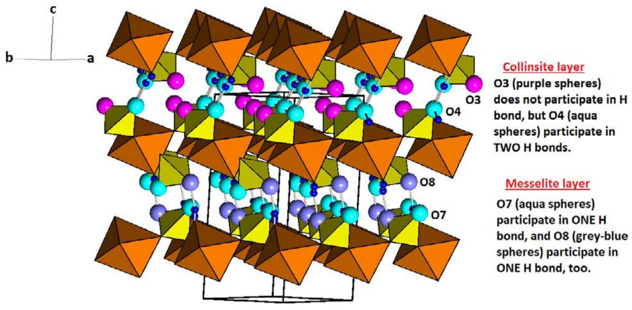

(c) Two layers in dondoellite = Collinisite layer + Messelite layer

FIG. 7. Comparison of the H-bonding schemes in collinsite, messelite, and dondoellite. The legend is the same as in Figure 4. Small blue spheres represent H atoms. For clarity, Ca atoms have been omitted.

TABLE 8. BOND-VALENCE SUMS FOR DONDOELLITE

	Ca1	Ca2	Fe	P1	P2	Sum
O1	0.211	0.136	0.338	1.224		1.904
O2	0.208	0.215	0.292	1.210		1.925
O3	0.302 0.261			1.347		1.909
O4	0.306			1.264		1.570
O5	0.196	0.261	0.287		1.219	1.961
O6	0.137	0.236	0.323		1.226	1.904
O7		0.279 0.233			1.248	1.760
O8		0.386			1.348	1.734
Ow9	0.306		0.403			0.709
Ow10		0.285	0.377			0.661
Sum	1.924	2.031	2.019	5.045	5.041	

Note: The bond valence sum for Fe was calculated based on ($0.87Fe^{2+} + 0.13Mg^{2+}$).

rise to a new structure type that is a combination of the Type A and Type B structures for materials with kröhnkite-type chains. In other words, both the collinsite- and messelite-type layers are required to form the dondoellite structure. The messelite-type layer alone, regardless of how it may stack [001], is not sufficient to produce the crystal structure of dondoellite and, as such, it cannot be strictly considered a polytype of the crystal structure of messelite. Bond-valence sums calculated using the parameters from Brese & O'Keeffe (1991) (Table 8) indicate that Ow9 and Ow10 are H_2O and O4 is substantially more under-bonded (1.570 v.u.) (two H-bond acceptors) than O7 (1.760 v.u.) and O8 (1.734 v.u.) (both being one H-bond acceptor).

It is worth noting that Frondel (1955) reported a mineral with both chemical and powder X-ray diffraction differing slightly from those for messelite, which was named "neomesselite", alluding to the mineral being the "new" equivalent for the then-discredited messelite. As the Ca/M^{2+} (M = Fe + Mn + Mg) ratio ranges from 1.10 to 1.81 for "neomesselite", which is significantly less than the ideal value of 2 for messelite, Frondel (1955) suggested that Ca and M^{2+} were "structurally equivalent" or disordered in "neomesselite" and proposed a chemical formula of $(Ca,Fe,Mn)_3(PO_4)_2{\cdot}2H_2O$ for it. Čech & Pedera (1958) re-examined "messelite" from the type locality (Messel, Germany) and concluded that the discreditation of messelite was in error and suggested that messelite be reinstated as the name of choice. Figure 8 compares powder X-ray diffraction patterns for messelite, "neomesselite", and dondoellite. The differences among them are evident, which, together with the marked difference in chemistry, rules out the likelihood that dondoellite is equivalent to the "neomesselite" of Frondel (1955).

According to the Raman spectroscopic study of minerals of the fairfieldite group, including messelite, by Frost (2009), the tentative assignments of major Raman bands for dondoellite are given in Table 9. The broad bands between 2860 and 3300 cm^{-1} are attributed to the O–H stretching vibrations and those around 1590 cm^{-1} to the H–O–H bending vibrations in H_2O. Similar broad bands were also observed for messelite by Frost (2009). The nature of the broad bands between 2250 and 2550 cm^{-1} is unclear. The bands between 900 and 1150 cm^{-1} are ascribable to the P–O stretching vibrations within the PO_4 group,

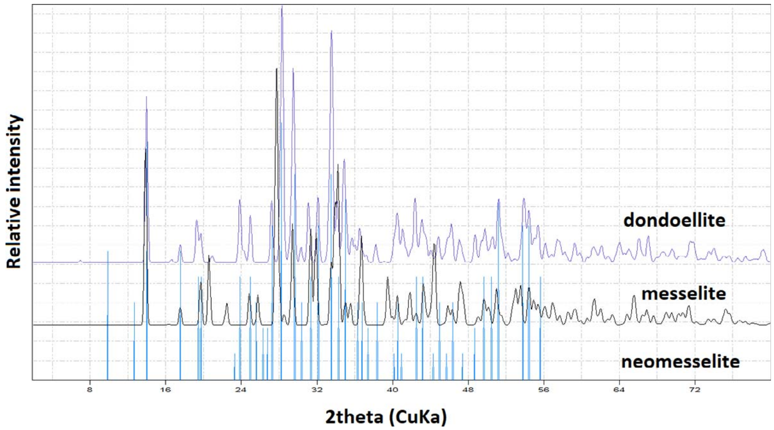

FIG. 8. The powder X-ray diffraction patterns for dondoellite, messelite, and neomesselite.The powder diffraction data for dondoellite and messelite were calculated from the structures of this study and Fleck & Kolitsch (2003), respectively, whereas those for neomesselite were taken from Frondel (1955).

TABLE 9. TENTATIVE ASSIGNMENT OF MAJOR RAMAN BANDS FOR DONDOELLITE

Bands (cm^{-1})		Assignment
2860–3300	very broad	O–H stretching vibrations in H_2O.
2280–2480	weak, broad	O–H···O interactions.
1590	very weak	H–O–H bending vibrations in H_2O.
900–1150	strong, sharp	P–O stretching vibrations within the PO_4 groups.
400–600	relatively strong	O–P–O bending vibrations within the PO_4 groups.
<400	weak	Rotational and translational modes of PO_4 tetrahedra, as well as the *M*–O (M^{2+} = Fe, Ca) interactions and lattice vibrational modes.

whereas those from 400 to 660 cm^{-1} are due to the O–P–O bending vibrations. The bands below 400 cm^{-1} are mainly associated with the rotational and translational modes of PO_4 tetrahedra, as well as the *M*–O (M^{2+} = Fe, Ca) interactions and lattice vibrational modes. For comparison, the Raman spectra of fairfieldite (R050539) and collinsite (R060140) from the RRUFF Project (http://rruff.info) were also plotted in Figure 3. The strong resemblance among the three spectra is apparent. Differences in peak intensities between the two spectra may result from differences in the orientations of the crystals used to collect the data.

In the classification for materials with kröhnkite-type chains (Fleck *et al*. 2002a), many Type A minerals (represented by collinsite) have polymorphs that belong to Type D (represented by roselite), such as talmessite *versus* wendwilsonite for $Ca_2Mg(AsO_4)_2 \cdot 2H_2O$, brandtite *versus* parabrandtite for $Ca_2Mn^{2+}(AsO_4)_2 \cdot 2H_2O$, roselite *versus* roselite-β for $Ca_2Co(AsO_4)_2 \cdot 2H_2O$, and gaitite *versus* zincroselite for $Ca_2Zn(AsO_4)_2 \cdot 2H_2O$. Interestingly, all these minerals with polymorphs are arsenates.

Messelite, which belongs to Type B (represented by fairfieldite), is the first phosphate with the kröhnkite-type chain that represents a polymorph (dondoellite). As such, the existence of dondoellite raises the question as to whether polymorphs of fairfieldite, $Ca_2Mn^{2+}(PO_4)_2 \cdot 2H_2O$, or collinsite, $Ca_2Mg(PO_4)_2 \cdot 2H_2O$, may also exist. In fact, Frondel (1955) noted that fairfieldite from Branchville, Connecticut, and Buckfield, Maine, have identical X-ray powder diffraction patterns but that these differ slightly from those of the fairfieldite from Newry, Maine, and Hagendorf, Bavaria. An unambiguous answer to this observation will require further detailed examinations of these materials with single-crystal X-ray structural analyses.

ACKNOWLEDGEMENTS

We are grateful for the constructive comments by Dr. Pietro Vignola. This study was funded by the Feinglos family and Mr. Michael M. Scott.

REFERENCES

BRESE, N.E. & O'KEEFFE, M. (1991) Bond-valence parameters for solids. *Acta Crystallographica* **B47**, 192–197.

BROTHERTON, P.D., MASLEN, E.N., PRYCE, M.W., & WHITE, A.H. (1974) Crystal structure of collinsite. *Australian Journal of Chemistry* **27**, 653–656.

ČECH, F. & PEDERA, K. (1958) Messlit aus den Phosphatnestern im Granit bei Pribyslavice (Bohmen) und das Messelitproblem. *Chemie der Erde* **19**, 436–449.

DOWNS, R.T., BARTELMEHS, K.L., GIBBS, G.V., & BOISEN, M.B., JR. (1993) Interactive software for calculating and displaying X-ray or neutron powder diffractometer patterns of crystalline materials. *American Mineralogist* **78**, 1104–1107.

FLECK, M., KOLITSCH, U., & HERTWECK, B. (2002a) Natural and synthetic compounds with kröhnkite-type chains: Review and classification. *Zeitschrift für Kristallographie* **217**, 435–443.

FLECK, M., HERTWECK, B., KOLITSCH, U., GIESTER, G., WILDNER, M., PRERN, M., & WOHLSCHLAGCR, A. (2002b) Crystal structures of the double salt dihydrates $K_2Cd(SeO_4)_2 \cdot 2H_2O$, $K_2Mn(SO_4)_2 \cdot 2H_2O$, $(NH_4)_2Cu(SeO_4)_2 \cdot 2H_2O$ and $KFeH(SO_4)_2 \cdot 2H_2O$. *Zeitschrift für Kristallographie* **217**, 242–248.

FLECK, M. & KOLITSCH, U. (2003) Natural and synthetic compounds with kröhnkite-type chains. An update. *Zeitschrift für Kristallographie* **218**, 553–567.

FRONDEL, C. (1955) Neomesselite and beta-roselite: Two new members of the fairfieldite group. *American Mineralogist* **40**, 828–833.

FROST, R.L. (2009) Raman and infrared spectroscopy of arsenates of the roselite and fairfieldite mineral subgroups. *Spectrochimica Acta Part A: Molecular and Biomolecular Spectroscopy* **71**, 1788–1794.

HERWIG, S. & HAWTHORNE, F.C. (2006) The topology of hydrogen bonding in brandtite, collinsite and fairfieldite. *Canadian Mineralogist* **44**, 1181–1196.

KOLITSCH, U. & FLECK, M. (2006) Third update on compounds with kröhnkite-type chains: The crystal structure of wendwilsonite [$Ca_2Mg(AsO_4)_2 \cdot 2H_2O$] and the new triclinic structure of synthetic $AgSc(CrO_4)_2 \cdot 2H_2O$ and $M_2Cu(Cr_2O_7)_2 \cdot 2H_2O$ (M=Rb, Cs). *European Journal of Mineralogy* **18**, 471–482.

MANDARINO, J.A. (1981) The Gladstone-Dale relationship: Part IV. The compatibility concept and its application. *Canadian Mineralogist* **19**, 441–450.

PEYTAVIN, S., AVINENS, C., COT, L., & MAURIN, M. (1974) Systematique structural des composes a anions tetrahedriques divalents de formule $M^{I}_2M^{II}(AB_4)_2 \cdot xH_2O$. *Revue de Chimie Minérale* **11**, 689–700.

ROBINSON, G.W., VAN VELTHUIZEN, J., ANSELL, H.G., & Sturman, B.D. (1992) Mineralogy of the Rapid Creek and Big Fish River area, Yukon Territory. *Mineralogical Record* **23**, 1–47.

SHELDRICK, G.M. (2015a) SHELXT – Integrated space-group and crystal structure determination. *Acta Crystallographica* **A71**, 3–8.

SHELDRICK, G.M. (2015b) Crystal structure refinement with SHELX. *Acta Crystallographica* **C71**, 3–8.

Received February 15, 2022. Revised manuscript accepted June 14, 2022.

This manuscript was handled by Associate Editor Frédéric Hatert and Editors Lee Groat and Andrew McDonald.